

Supporting information

Graphene Growth under *Knudsen* Molecular Flow on Confined Catalytic Metal Coil

Hyojin Bong[†], *Sae Byeok Jo*[†], *Boseok Kang*, *Seong Kyu Lee*, *Hyun Ho Kim*, *Seunggoo Lee*, *Kilwon Cho*^{*}

[[†]] H.Bong and S.B. Jo contributed equally to this work.

Send correspondence to

Kilwon Cho (kwcho@postech.ac.kr),

Department of Chemical Engineering, Pohang University of Science and Technology,
Pohang 790-784, Korea.

Relative diffusivity of confined system

Diffusivity of gases, in the open non-stacked system, (D_A) is defined as,¹

$$D_A = \frac{\lambda}{3} \sqrt{\frac{8k_B K}{\pi M_A}}$$

where,

λ = mean free path

k_B = Boltzmann constant,

K = thermodynamic temperature,

M_A = molecular weight of gas.

For *Knudsen* diffusion, λ should be replaced with system dimension, L . The relative diffusivity of confined system of gases (D_K) can now be defined as,

$$D_K = \frac{L}{3} \sqrt{\frac{8k_B K}{\pi M_A}} = \frac{D_A}{Kn}$$

where,

L = gap size

$Kn = \lambda / L = Knudsen$ number.

¹ Welty, James R. Wicks, Charles E. Wilson, Robert E. Rorrer, Gregory L. (2008). *Fundamentals of Momentum, Heat and Mass Transfer* (5th ed.). Hoboken: John Wiley and Sons.

Table S1. Calculated *Knudsen* number ($Kn = \lambda/L$, $\lambda = 119 \mu\text{m}$) at various gap sizes, and flow regimes according to *Knudsen* number.

Gap size (L)	Kn	Flow regime
135 nm (stack)	881.5	Free molecular flow ($Kn > 10$)
585 nm	203.4	
30 μm	3.53	Transition flow ($0.1 < Kn < 10$)
600 μm	0.18	
1.2 mm	0.09	Slip flow ($0.001 < Kn < 0.1$)

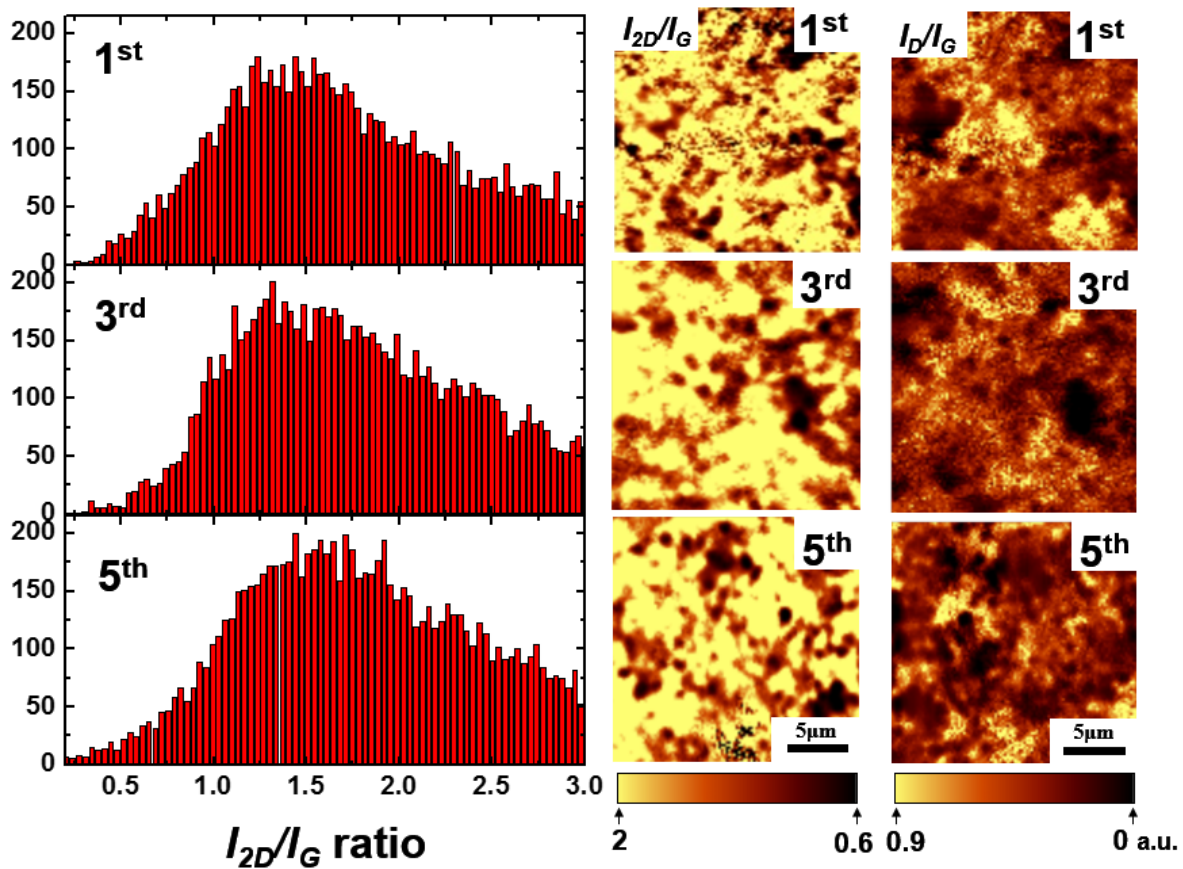


Figure S1. Statistical distribution and Raman 2D-mapping (I_{2D}/I_G and I_D/I_G area $400 \mu\text{m}^2$) of the graphene films obtained from the multi-layer stacked substrates, 1st, 3rd, and 5th layers.

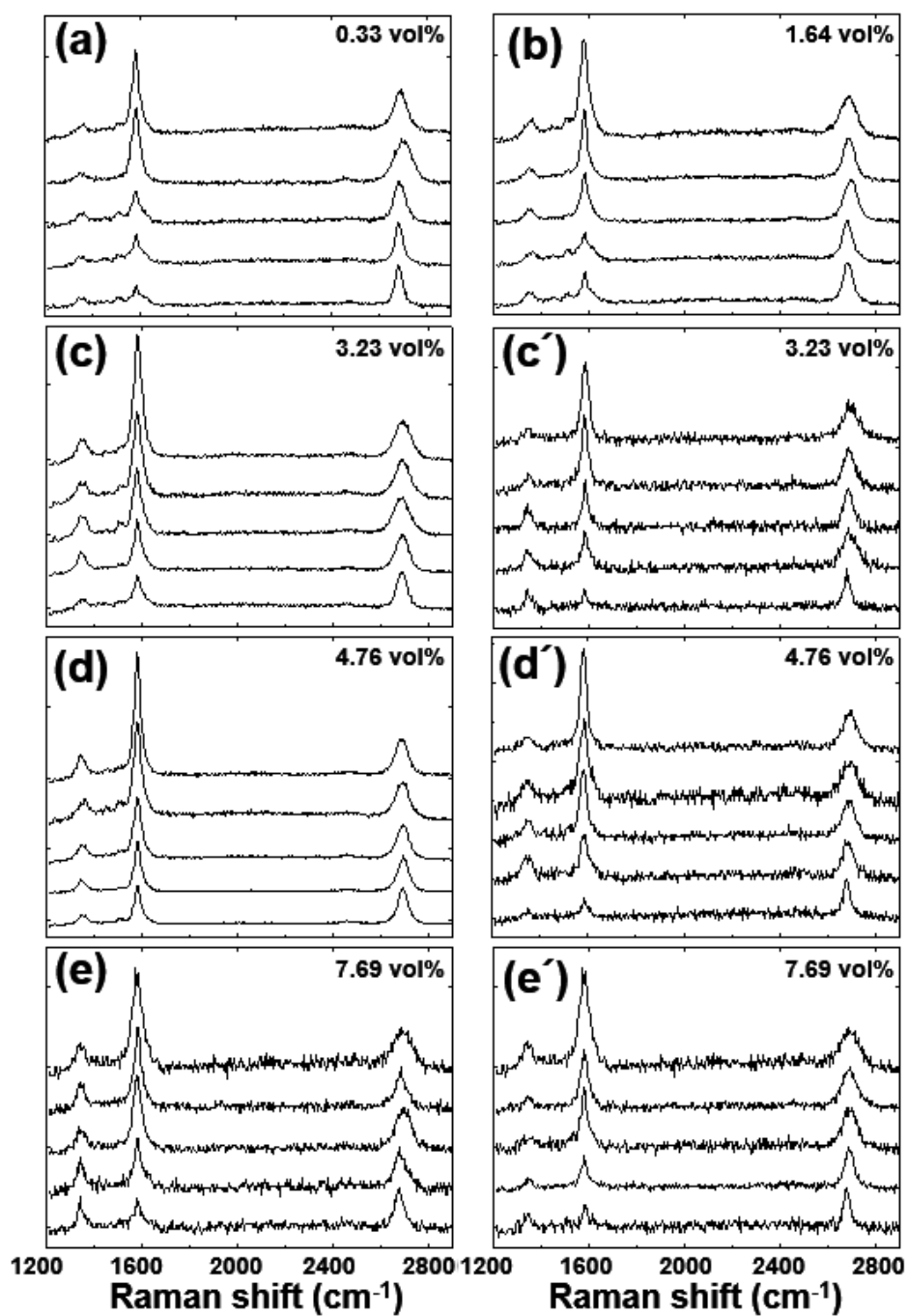
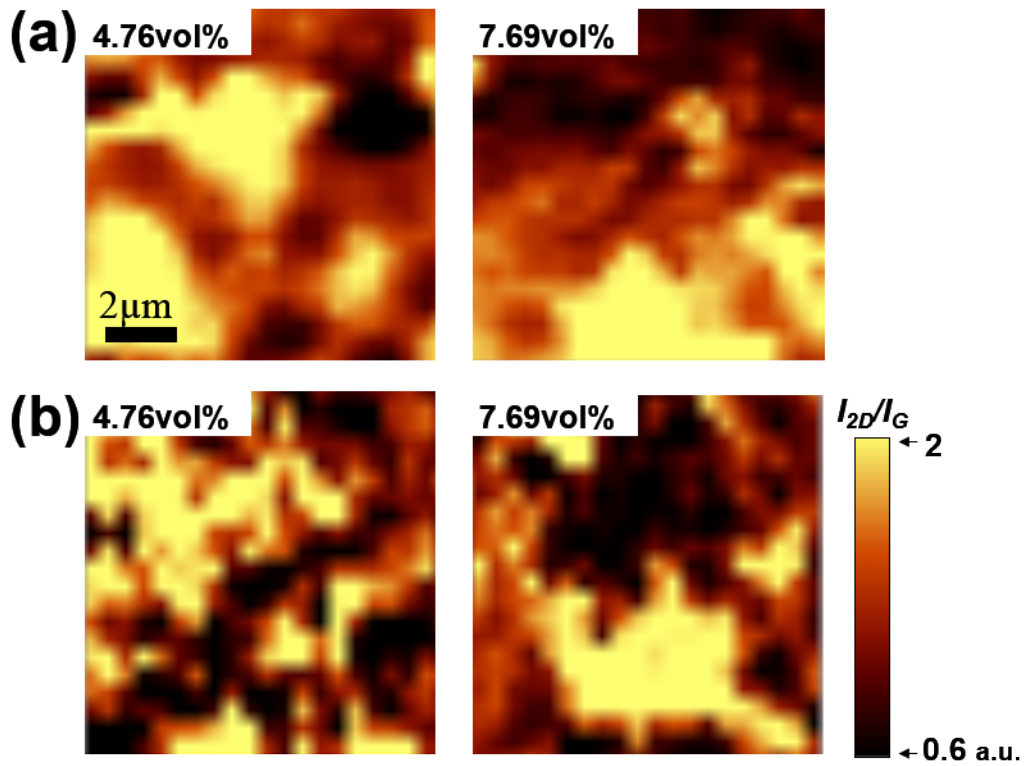


Figure S2. Raman spectra of the graphene films obtained (a) ~ (e) from the stacked systems and (c') ~ (e') from the non-stacked system on the SiO₂/Si substrates.



CH ₄ concentration	4.76 vol%		7.69 vol%	
	Mono-layer	Bi-layer	Mono-layer	Bi-layer
Stacked system	25.3 %	51.4 %	18.9 %	35.5 %
Non-stacked system	22.1 %	42.1 %	19.3 %	31.0 %

Figure S3. The Raman mapping images of the graphene films (I_{2D}/I_G ratio, area $100 \mu\text{m}^2$). (a) CH₄ concentrations are 4.76 and 7.69 vol% in the stacked system. (b) CH₄ concentrations are 4.76 and 7.69 vol% in the non-stacked system. Table shows the percentages of the monolayer and bi-layer parts obtained from each graphene film.

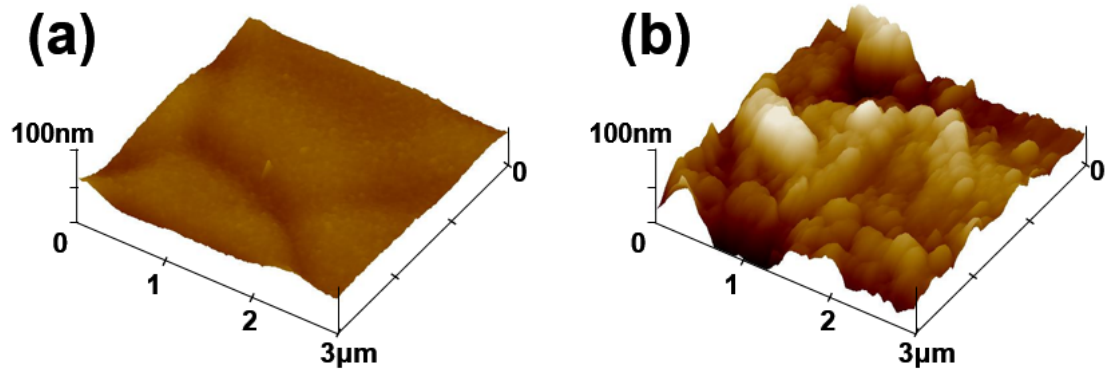
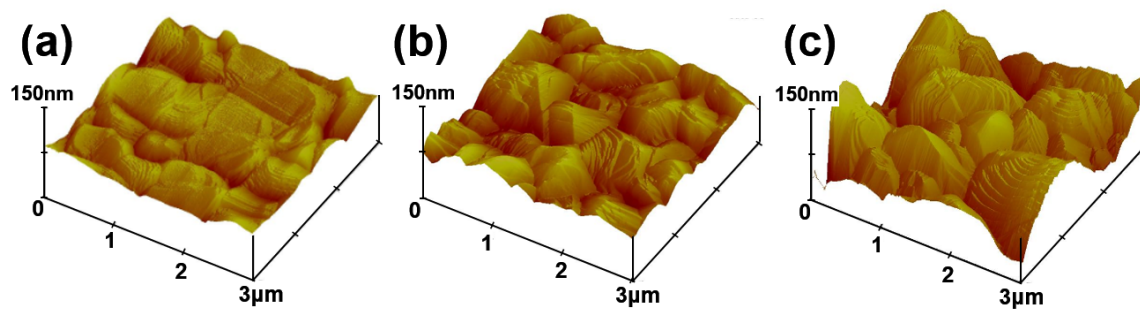


Figure S4. The height of (a) the back side of the upper substrate (≈ 65 nm) and (b) the SUS surface (≈ 130 nm).



Gap size	135 nm (stacked system)	30 μm	1.2 mm	Non-stacked system
RMS	8.7 nm	17.4 nm	24.1 nm	23.8 nm
Max. height	69.7 nm	137.2 nm	170.3 nm	270.9 nm

Figure S5. AFM images of heat-treated Ni surfaces under a H_2/Ar atmosphere for various gap sizes of (a) 135 nm (stacked system), (b) 30 μm , and (c) 1.2 mm.

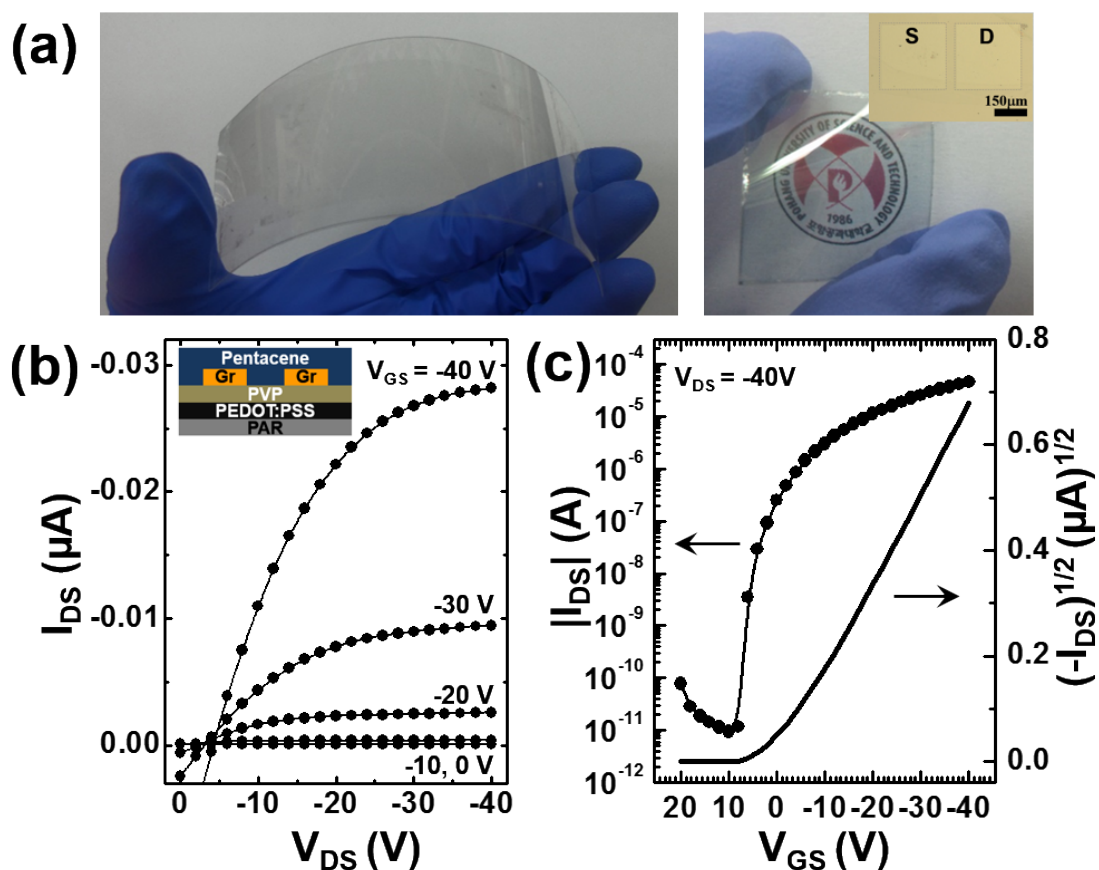


Figure S6. Demonstration of graphene-based large area flexible transparent conducting films (TCFs) and flexible OFETs. (a) Photographs of (left) flexible TCFs (8cm \times 3cm) and (right) pentacene-based OFET array on flexible PAR substrates using pattern-transferred graphene as source/drain electrodes. Inset shows optical image of graphene electrode (L = 50 μ m, W = 200 μ m). (b) Output characteristics and (c) transfer characteristics of OFETs. Inset in (b) shows schematic diagram of a cross section of FETs.

For flexible TCF demonstrations, 8 cm \times 3 cm (width \times length) Ni/SUS film was roll-stacked to give a catalytic coil with dimension of 1 cm \times 3 cm (diameter \times length) as shown in Figure S5a. The graphene was synthesized under CH₄ concentration of 1.64 vol% on the roll-stacked coil in a closed CVD chamber and then was transferred to PAR substrate by

conventional wet-transfer method as described in the experimental section. The average R_S of TCF was 1.51 ± 0.29 k Ω /sq.

Pentacene-based OFETs were characterized by measuring the output and transfer characteristics of the devices, as shown in Figure S5b ~ c. The transfer characteristics were used to calculate the field-effect mobility in the saturation regime using the relationship,

$$I_{DS} = \frac{\mu C_i W}{2L} (V_{GS} - V_{th})^2$$

where W and L are the channel width and length, respectively, C_i is the specific capacitance of the gate dielectric, and μ is the field-effect mobility. The average field-effect mobilities obtained from the transfer curve were 0.51 cm²/Vs and the device showed high mechanical stability.

Fabrication of organic field effect transistor (OFET): Graphene electrode based OFET devices were built on flexible plastic substrates using polyarylate (PAR, Ferrania Technologies). A gate electrode was spin-casted onto the PAR films using a water-based ink of the conducting polymer that is poly(3,4-ethylenedioxythiophene) doped with polystyrene sulfonic acid (PEDOT/PSS, Baytron P from Bayer AG). Then, a gate dielectric was deposited by spin-casting onto the PAR film using a mixture of poly-4-vinylphenol (PVP, $M_w = 20,000$ g/mol) and poly(melamine-co-formaldehyde), methylated (PMF, $M_w = 511$ g/mol) in dimethylformamide solution. The film was heat-treated to cross-link the gate dielectric layer for 1 h at 180 °C in a vacuum oven. UV lithography method was used for patterning the graphene films as source/drain electrodes. By etching RIE plasma (250W, 60s), the patterned graphene electrodes were fabricated and had the defined channel lengths and widths as $L = 30, 50$ μ m; $W = 200$ μ m. Finally, 50 nm thick pentacene as an active layer for OFETs were thermally evaporated onto the films under vacuum ($\sim 10^{-6}$ Torr).